

Discrete-Continuous Smoothing and Mapping

Kevin J. Doherty*, Ziqi Lu, Kurran Singh, and John J. Leonard

Computer Science and Artificial Intelligence Laboratory,
Massachusetts Institute of Technology,
Cambridge, MA 02139, USA

* Corresponding author. Email: kjd@csail.mit.edu

Abstract—We describe a general approach to smoothing and mapping with a class of *discrete-continuous factor graphs* commonly encountered in robotics applications. While there are openly available tools providing flexible and easy-to-use interfaces for specifying and solving optimization problems formulated in terms of either discrete or continuous graphical models, at present, no similarly general tools exist enabling the same functionality for *hybrid* discrete-continuous problems. We aim to address this problem. In particular, we provide a library, DC-SAM, extending existing tools for optimization problems defined in terms of factor graphs to the setting of discrete-continuous models. A key contribution of our work is a novel solver for efficiently recovering approximate solutions to discrete-continuous optimization problems. The key insight to our approach is that while joint inference over continuous and discrete state spaces is often hard, many commonly encountered discrete-continuous problems can naturally be split into a “discrete part” and a “continuous part” that can individually be solved easily. Leveraging this structure, we optimize discrete and continuous variables in an alternating fashion. In consequence, our proposed work enables straightforward representation of and approximate inference in discrete-continuous graphical models. We also provide a method to recover the uncertainty in estimates of both discrete and continuous variables. We demonstrate the versatility of our approach through its application to three distinct robot perception applications: point-cloud registration, robust pose graph optimization, and object-based mapping and localization.

SUPPLEMENTAL MATERIAL

The DC-SAM library is currently available at <https://www.github.com/MarineRoboticsGroup/dcsam>. Several components of DC-SAM are presently undergoing migration into GTSAM at <https://www.github.com/borglab/gtsam>.

I. INTRODUCTION

Probabilistic graphical models have become the dominant representational paradigm in robot perception applications, appearing in a wide range of important estimation problems. This formalism has led to the development of numerous algorithms and software libraries, such as GTSAM [10], which provide flexible and modular languages for specifying and solving optimization problems defined by these models (typically in terms of *factor graphs*). Among the models relevant to robotics applications, *discrete-continuous graphical models* capture a great breadth of key problems arising in robot perception, task and motion planning [16, Sec 3.2], and navigation, including data association, outlier rejection, and semantic simultaneous localization and mapping (SLAM) [39] (see Figure 1). Despite

the importance of these models, while *ad hoc* solutions have been proposed for *particular* problem instances, at present there is no off-the-shelf approach for hybrid problems that is either as general or as easy-to-use as similar methods for their continuous-only or discrete-only counterparts. This is the problem that we consider in this paper.

Our key insight is that in many instances, while optimizing over discrete and continuous variables jointly is hard (see e.g. [25, Ch. 14]), if we fix either the discrete or continuous variables, local optimization of the other set is easy. Continuous optimization can be performed using smooth, gradient-based methods, while discrete optimization can be performed *exactly* for a fixed assignment to the continuous variables by means of standard max-product variable elimination [25, Ch. 13]. Moreover, this approach naturally extends many of the additional desired capabilities of an inference approach in robotics applications, such as incremental computation [24] and uncertainty estimation (cf. [23]) to the hybrid setting.

Our contributions are as follows: From a robotics science standpoint, we show that by leveraging the conditional independence structure of hybrid factor graphs commonly encountered in robotics problems, efficient local optimization can be performed using alternating optimization, which we prove guarantees monotonic improvement in the objective. Because our approach naturally respects the incremental structure of many such problems, it easily scales to thousands of discrete variables *without* the need to prune discrete assignments. From a systems standpoint, our discrete-continuous smoothing and mapping (DC-SAM) library extends existing GTSAM tools by adding (1) explicit constructions for hybrid discrete-continuous factors, (2) a new solver capable of computing approximate solutions to the corresponding estimation problems, and (3) an approach for recovering uncertainties associated with solutions to these problems which does not depend on the solver we employ (and therefore is likely to be of independent interest). To the best of our knowledge, these are the first openly-available tools for general discrete-continuous factor graphs encountered in robotics applications. We demonstrate the application of our methods to three disparate robot perception problems: point-cloud registration, pose graph optimization, and semantic SLAM. In the former two cases, our general approach naturally recovers well-known solutions. In semantic SLAM, our method produces high-quality trajectory and semantic map estimates in real-time.

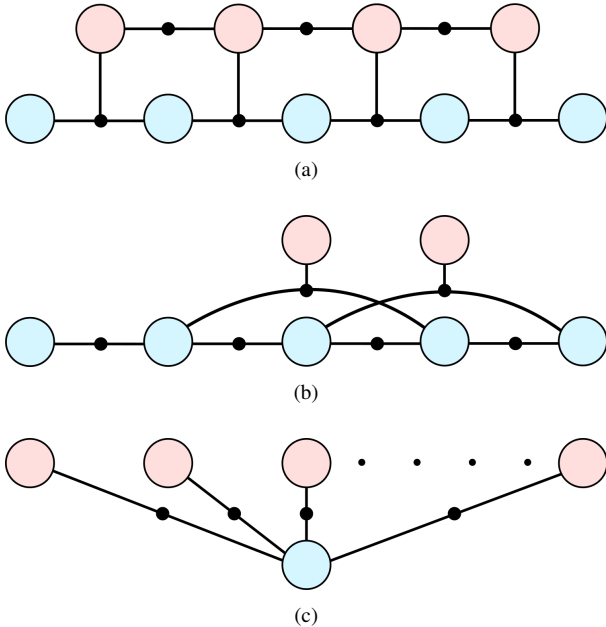


Fig. 1: **Discrete-continuous factor graphs in robotics.** Factor graphs modeling several relevant discrete-continuous robot perception problems. Discrete variable nodes are colored red, continuous variable nodes are blue, and factor nodes are black. (a) Switching systems: discrete states control the evolution of a continuous process. (b) Outlier rejection: discrete inlier/outlier variables control whether a subset of untrusted measurements should be used in estimating continuous variables. (c) Point-cloud registration: discrete variables represent correspondences and the continuous variable is the relative transformation from a source to target point-cloud.

II. RELATED WORK

The problem of inference in discrete-continuous graphical models arises in many domains and intersects a number of communities, even within the field of robotics. Since our focus in this paper will be on applications in robot perception, we primarily discuss related works in these settings. However, Dellaert [11] gives a discussion of these models in the context of broader robotics applications. The interested reader may also refer to Koller and Friedman [25, Ch. 14] for a discussion of computational hardness, inference techniques, and a detailed review of literature on the general problem of inference in hybrid models. Finally, while we discuss our alternating minimization approach in relation to existing methods, it is important to note: the mere availability of a consistent framework in which these solutions could be implemented enables practitioners to compare different approaches without the need to develop the additional scaffolding usually required to adapt an existing method.

A. Multi-Hypothesis Methods

The class of approaches addressing hybrid estimation by enumerating and systematically pruning solutions to the discrete states are referred to as *multi-hypothesis methods*. These methods appeared in classical detection and tracking problems [36] and early SLAM applications [8]. In the event that bounds

on solution quality can be attained, the “branch and bound” paradigm can be used to prune solutions without the risk of eliminating optimal solutions, which is commonly applied in the setting of data association (e.g. [31, 48]).

MH-iSAM2 [20] extends the capabilities of iSAM2 [24] to the case where measurements between continuous variables may have ambiguity, which can be represented by the introduction of discrete hypotheses. It does so by retaining a hypothesis tree, which the authors show can be constructed and updated in an incremental fashion, like iSAM2, making the solver efficient. The types of ambiguities they consider can all be represented as factors in a factor graph where the discrete variables are all conditionally independent. This limits application to scenarios where individual discrete variables can be *decoupled*. However, correlations between discrete variables may arise in problem settings as diverse as switching systems (Figure 1; see also [22]), outlier rejection¹, and as we explore in Section V-C, semantic SLAM. Furthermore, in order to retain computational efficiency, MH-iSAM2, like all multi-hypothesis methods, must prune hypotheses, which risks the deletion of hypotheses that would have later become high-probability modes.

iMHS [22] takes a qualitatively similar approach to MH-iSAM2 to perform smoothing in discrete-continuous models, effectively running multiple smoothers in parallel. Their approach extends to the setting where correlations among discrete variables are present. Like MH-iSAM2, however, the efficiency of iMHS rests on the ability to prune incorrect modes.

B. Non-Gaussian Inference

Several approaches have been presented which consider the general issue of *non-Gaussian* inference in graphical models with application to robot perception. FastSLAM [30] is an approach to filtering in SLAM with non-Gaussian models based on particle filters. In particular, a set of particles representing the current state of a robot is retained, and each particle independently samples associations from a distribution over hypotheses.

Multimodal iSAM (mm-iSAM) [15] is an approach to incremental non-Gaussian smoothing for continuous-valued variables which uses nonparametric belief propagation [43]. In situations where discrete variables can be efficiently eliminated through marginalization to produce a problem exclusively involving continuous states, mm-iSAM can approximate the posterior marginals over the remaining continuous variables. NF-iSAM [21] similarly addresses the issue of smoothing in non-Gaussian graphical models, but represents the posterior using normalizing flows. Like mm-iSAM, by marginalizing the discrete variables, NF-iSAM can capture certain discrete ambiguities (e.g. unknown data association).

In contrast, our work is concerned with the problem of maximum *a posteriori* (MAP) estimation; i.e. rather than

¹Though we do not explore the issue of outlier rejection problems with correlations, the interested reader may see Lajoie et al. [26] for a formulation in the setting of SLAM.

estimating distributions over the variables of interest, we seek a single point estimate. While we provide a mechanism for recovering approximate marginals from an estimate, the uncertainties provided by non-Gaussian inference methods can be substantially richer. However, considering a somewhat more restricted problem setting affords us considerable benefits in terms of computational expense. Prior works that have considered MAP estimation in non-Gaussian models (e.g. [34, 38]) do so by marginalizing out the discrete variables and using smooth optimization techniques on the resulting continuous estimation problem; consequently, they do not permit the explicit estimation of discrete states, as we consider here.

C. Existing Tools

Several existing solvers perform optimization with models that can be represented in terms of factor graphs. Ceres [2] and g2o [19] provide nonlinear least-squares optimization tools which are suitable for robotics applications; however, they are not suitable for inference in general factor graphs of the kind encountered in Figure 1. In addition to these tools, GTSAM [10] provides incremental nonlinear least-squares solvers, like iSAM2 [24], and tools for representing and solving discrete factor graphs; it is for these reasons that we choose to extend the capabilities of GTSAM to the setting of hybrid, discrete-continuous models. Finally, Caesar.jl [7] implements mm-iSAM [15] and therefore supports approximate, incremental non-Gaussian inference over graphical models commonly encountered in SLAM; this includes discrete-continuous models in scenarios where discrete variables can be eliminated through marginalization to produce a problem exclusively involving continuous variables.

III. BACKGROUND AND PRELIMINARIES

A *factor graph* $\mathcal{G} \triangleq \{\mathcal{V}, \mathcal{F}, \mathcal{E}\}$ with factor nodes $f_k \in \mathcal{F}$, variable nodes $v_i \in \mathcal{V}$, and edges \mathcal{E} is a graphical representation of a product factorization of a function. In our setting, we are interested in determining the most probable assignment to a set of discrete variables D and continuous variables C given a set of measurements Z . Under the assumption that each measurement z_k is independent of all others given the quantities it relates, we can decompose the posterior $p(C, D | Z)$ into a product of measurement factors f_k , each of which depends only on a small subset of variables \mathcal{V}_k :

$$p(C, D | Z) \propto \prod_k f_k(\mathcal{V}_k), \quad (1)$$

$$\mathcal{V}_k \triangleq \{v_i \in \mathcal{V} \mid (f_k, v_i) \in \mathcal{E}\},$$

where each factor f_k is in correspondence with either a measurement likelihood of the form $p(z_k | \mathcal{V}_k)$ or a prior $p(\mathcal{V}_k)$. From (1), the posterior $p(C, D | Z)$ can be decomposed into factors f_k of three possible types: *discrete* factors $f_k(D_k)$ where $D_k \subseteq D$, *continuous* factors $f_k(C_k)$, $C_k \subseteq C$, and *discrete-continuous* factors $f_k(C_k, D_k)$. In turn, the maximum

a posteriori inference problem can be posed as follows:

$$\begin{aligned} C^*, D^* &= \operatorname{argmax}_{C,D} p(C, D | Z) \\ &= \operatorname{argmax}_{C,D} \prod_k f_k(\mathcal{V}_k) \\ &= \operatorname{argmin}_{C,D} \sum_k -\log f_k(\mathcal{V}_k). \end{aligned} \quad (2)$$

That is to say, we can maximize the posterior probability $p(C, D | Z)$ by minimizing the negative log posterior, which in turn decomposes as a summation. Though the theoretical aspects of the methods we propose are quite general, in application we will primarily be concerned with factor graphs in which maximum likelihood estimation (or maximum *a posteriori* inference) can be represented in terms of a nonlinear least-squares problem, which permits the application of incremental nonlinear least-squares solvers like iSAM2 [24].² In particular, we consider discrete-continuous factors $f_k(C_k, D_k)$ admitting a description as:

$$\begin{aligned} -\log f_k(C_k, D_k) &= \|r_k(C_k, D_k)\|_2^2, \\ C_k &\subseteq C, \quad D_k \subseteq D, \end{aligned} \quad (3)$$

where r_k is typically nonlinear in C and first-order differentiable with respect to C , and the equality may be up to a constant independent of C and D . Likewise, we consider factors involving only continuous variables admitting an analogous representation. We place no restriction on discrete factors.

IV. OVERVIEW OF THE APPROACH

The following subsections describe our approach to solving optimization problems of the form in (2). In Section IV-A, we outline our core alternating minimization procedure and prove that our approach enjoys monotonic descent guarantees. In Section IV-B, we describe how our approach can easily benefit from existing incremental optimization techniques to efficiently solve large-scale estimation problems. Finally, in Section IV-C, we consider the issue of recovering *uncertainties* for the estimates provided by our method.

A. Alternating Minimization

In the most general cases, the MAP inference problem in (2) is computationally intractable [25]. Indeed, even the purely continuous estimation problems arising in robot perception are typically NP-hard, including rotation averaging and pose-graph SLAM [39]. Despite this, smooth (local) optimization methods often perform quite well on such problems, both in their computational efficiency (owing to the fact that gradient computations are typically inexpensive) and quality of solutions when a good initialization can be supplied. However, even if we assume the ability to efficiently solve continuous estimation problems, the introduction of discrete variables complicates matters considerably: in the worst-case, solving

²This turns out not to be particularly restrictive; as demonstrated in Rosen et al. [38, Theorem 1], any factor which is positive and bounded admits an equivalent representation in terms of a nonlinear least-squares cost function for the purposes of optimization.

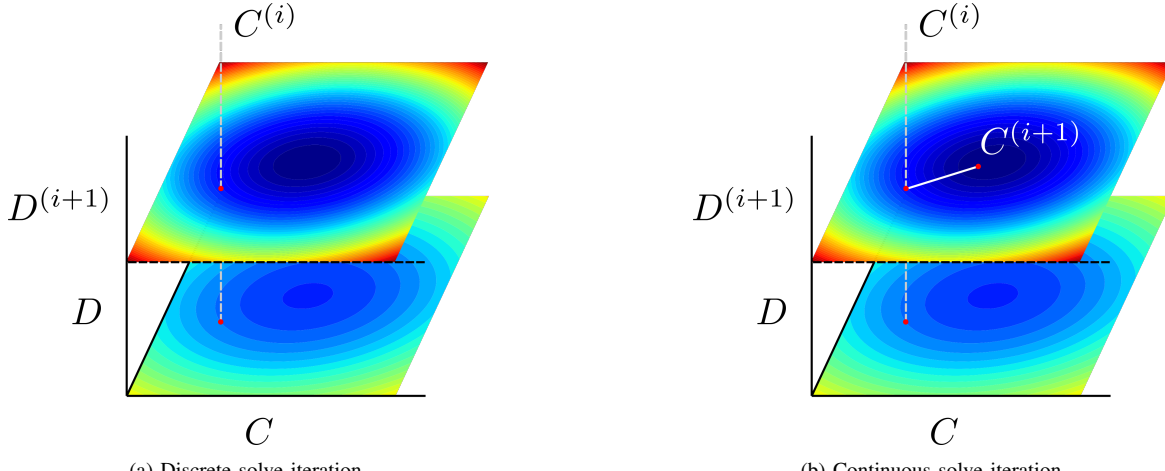


Fig. 2: **Overview of a single iteration of optimization.** (a) First, given an initial iterate $C^{(i)}$ we solve exactly for the optimal assignment to the discrete variables using max-product elimination. (b) Next, given the latest assignment to the discrete variables, we update the continuous variables (e.g. using a trust-region method [37]). Color depicts the objective value of a solution, ranging from low cost (blue) to high cost (red).

for the joint MAP estimate globally requires that for each assignment to the discrete states we solve a continuous optimization subproblem, and discrete state spaces grow *exponentially* in the number of discrete variables under consideration. Consequently, efficient approximate solutions are needed.

Our key insight is that we can leverage the conditional independence structure of the factor graph model to develop an efficient local inference method. To motivate our approach, we first observe that if we fix any assignment to the discrete states, the only variables remaining are continuous and approximate inference can be performed efficiently using smooth optimization techniques. In this sense, if we happened to know the assignment to the discrete variables, continuous optimization becomes “easy.” On the other hand, if we fix an estimate for the continuous variables, we are left with an optimization problem defined over a discrete factor graph which can be solved to global optimality using max-product variable elimination, but in the worst case may still require exploration of *exponentially many* discrete states. However, it turns out that for many commonly encountered problems, we can often do much better than the worst case.

In particular, consider a partition of the discrete states into mutually exclusive subsets $D_j \subseteq D$ which are *conditionally independent* given the continuous states:

$$p(D | C, Z) \propto \prod_j p(D_j | C, Z). \quad (4)$$

It is straightforward to verify from the mutual exclusivity of each set D_j that the problem of optimizing the conditional in (4) then breaks up into subproblems involving each D_j :

$$\max_D p(D | C, Z) \propto \prod_j \left[\max_{D_j} p(D_j | C, Z) \right]. \quad (5)$$

Critically, we have exchanged computation of the maximum of the product with the product of each maximum computed

independently. In cases where the discrete states decompose into particularly small subsets ($|D_j| \ll |D|$), inference may be carried out efficiently. Many hybrid optimization problems encountered in robotics admit such advantageous conditional independence structures. For example, Figures 1b and 1c, depicting robust pose graph optimization and point-cloud registration, respectively, admit a decomposition of the form in equation (4) where each subset D_j contains only *a single discrete variable*. Moreover, some discrete factor graphs do not decompose quite so drastically after conditioning on continuous states, but may still permit efficient inference. For example, Figure 1a depicts a switching system in which, after conditioning on the continuous variables, the resulting discrete graph is a hidden Markov model, for which the most probable assignment to the discrete states can be computed in polynomial time using the Viterbi algorithm [47].

In turn, we will use these ideas to construct an algorithm for efficiently producing solutions to problems of the form in (2). Consider the negative log posterior, defined as:

$$\mathcal{L}(C, D) \triangleq -\log p(C, D | Z). \quad (6)$$

From (2), the joint optimization problem of interest can be formulated as:

$$C^*, D^* = \underset{C, D}{\operatorname{argmin}} \mathcal{L}(C, D). \quad (7)$$

Our alternating minimization approach, depicted in Figure 2, proceeds as follows: first, fix an initial iterate $C^{(i)}$. Then, we aim to solve the following subproblems:

$$D^{(i+1)} = \underset{D}{\operatorname{argmin}} \mathcal{L}(C^{(i)}, D) \quad (8a)$$

$$C^{(i+1)} = \underset{C}{\operatorname{argmin}} \mathcal{L}(C, D^{(i+1)}). \quad (8b)$$

We may then repeat (8a) and (8b) until the relative decrease in $\mathcal{L}(C, D)$ is sufficiently small or we have reached a maximum

desired number of iterations. Finding minimizers for the subproblems (8a) and (8b) may still be challenging. Fortunately, one need not be able to find a minimizer for the subproblems (8a) and (8b) in order for our approach to enjoy monotonic improvements to the objective value. In particular, we require that at each iteration, the following hold as invariants:

$$\mathcal{L}(C^{(i)}, D^{(i+1)}) \leq \mathcal{L}(C^{(i)}, D^{(i)}) \quad (9a)$$

$$\mathcal{L}(C^{(i+1)}, D^{(i+1)}) \leq \mathcal{L}(C^{(i)}, D^{(i+1)}). \quad (9b)$$

It is clear that if we do indeed recover minimizers for each subproblem in (8a) and (8b) then these invariants hold. For the discrete subproblem, this can be ensured by using the max-product algorithm to compute the optimal assignment, and, for instance, by using a line search method in the case of the continuous subproblem [37]. In turn, we obtain the following proposition:

Proposition 1. *Let $\mathcal{L}(C, D)$ be the objective to be minimized, with initial iterate $C^{(0)}, D^{(0)}$. Suppose that at each iteration, the discrete update satisfies the descent criterion in (9a) and likewise for the continuous update in (9b). Then, the estimates $C^{(i)}, D^{(i)}$ obtained by alternating optimization satisfy:*

$$\mathcal{L}(C^{(0)}, D^{(0)}) \geq \mathcal{L}(C^{(1)}, D^{(1)}) \geq \dots \geq \mathcal{L}(C^{(T)}, D^{(T)}). \quad (10)$$

That is, this procedure ensures monotonic improvement in the objective.

Proof: Fix an initial iterate $(C^{(i)}, D^{(i)})$. By hypothesis, after a discrete update, we have $\mathcal{L}(C^{(i)}, D^{(i+1)}) \leq \mathcal{L}(C^{(i)}, D^{(i)})$ (from (9a)). Consequently, the updated assignment comprised of the pair $(C^{(i)}, D^{(i+1)})$ is *at least as good* as the previous assignment. By the same reasoning, performing a subsequent continuous update gives a pair $(C^{(i+1)}, D^{(i+1)})$ satisfying $\mathcal{L}(C^{(i+1)}, D^{(i+1)}) \leq \mathcal{L}(C^{(i)}, D^{(i+1)})$ (from (9b)). Combining these inequalities, we have:

$$\mathcal{L}(C^{(i+1)}, D^{(i+1)}) \leq \mathcal{L}(C^{(i)}, D^{(i+1)}) \leq \mathcal{L}(C^{(i)}, D^{(i)}). \quad (11)$$

The above chain of inequalities holds for all i , completing the proof. ■

B. Online, Incremental Inference

Many robotics problems naturally admit *incremental* solutions wherein new information impacts only a small subset of the states we would like to estimate. Because our alternating minimization approach relies only upon the ability to provide an improvement in each of the *separate* discrete and continuous subproblem steps, we can rely on existing techniques to solve these problems in an incremental fashion. In particular, in the continuous optimization subproblem, we use iSAM2 [24] to refactor the graph containing continuous variables into a *Bayes tree*, permitting incremental inference of the continuous variables. Similarly, owing to the discrete factorization in (4), if, for example, we introduce new discrete variables which are conditionally independent of all previous discrete states given the current continuous state estimate, we

are able to solve for the most probable assignment to these variables *without* the need to recompute solutions for previously estimated variables. In turn, we are able to efficiently solve online inference problems, as we demonstrate in Section V-C, in which we produce solutions to online SLAM problems in real-time.

C. Recovering Marginals

Uncertainty representation is important in many applications of robot perception. DC-SAM supports recovery of approximate marginal distributions for discrete and continuous variables. For continuous variables, we use the *Laplace approximate* [4, Sec. 4.4] adopted by several nonlinear least-squares solvers (Ceres, g2o, and GTSAM). In particular, we fix a linearization point for the continuous variables (and a current estimate for discrete variables) and compute an approximate linear Gaussian distribution centered at this linearization point. For discrete variables, we fix an assignment to the continuous variables and compute the exact discrete marginals conditioned on this linearization point using sum-product variable elimination [25, Ch. 9-10]. The marginals we recover, then are:

$$p(D_j | \hat{C}, Z) = \sum_{D \setminus D_j} p(D | \hat{C}, Z), \quad D_j \subseteq D, \quad (12a)$$

$$p(C_j | \hat{D}, Z) = \int_{C \setminus C_j} p(C | \hat{D}, Z), \quad C_j \subseteq C. \quad (12b)$$

The reason for this approach is that in the most general settings, the number of posterior modes captured by a particular (discrete-continuous) factor graph can grow combinatorially. Recovering the exact marginals can easily become intractable. In contrast, by making use of the conditional factorization in (4), solving for the discrete marginals in (12a) is often tractable.³ Notably, our approach to marginal recovery does not require that one use the alternating minimization strategy outlined in Section IV-A; any method of providing an estimate (\hat{C}, \hat{D}) will suffice.

The continuous marginals in (12b) are estimated using the Laplace approximation [23]. In our derivation, it will be convenient to consider the continuous states as a vector $C \in \mathbb{R}^d$. Assume that the point (\hat{C}, \hat{D}) is a critical point of the continuous subproblem (8b), i.e. $\nabla \mathcal{L}(C, \hat{D})|_{\hat{C}} = 0$. Then consider a Taylor expansion of the objective $\mathcal{L}(C, \hat{D})$ about the point \hat{C} :

$$\mathcal{L}(C, \hat{D}) \approx \mathcal{L}(\hat{C}, \hat{D}) - \frac{1}{2} A (C - \hat{C}), \quad (13)$$

with the $d \times d$ Hessian matrix A defined as:

$$A \triangleq -\nabla^2 \mathcal{L}(C, \hat{D})|_{\hat{C}}. \quad (14)$$

³It is also interesting to note that the discrete marginals we recover are *exactly* the “weights” computed in the expectation step of the well-known *expectation-maximization* (EM) algorithm [13].

Exponentiating both sides of (13) and appropriately normalizing the result gives the linear Gaussian approximation:

$$p(C \mid \hat{D}, Z) \approx \frac{|A|^{1/2}}{(2\pi)^{d/2}} \exp \left\{ -\frac{1}{2} \|C - \hat{C}\|_{A^{-1}}^2 \right\}, \quad (15)$$

where $\|c\|_{A^{-1}}$ denotes the Mahalanobis norm $\sqrt{c^\top A c}$. When all factors involving continuous variables take the form in (3), the locally linear approximation of \mathcal{L} about \hat{C} admits a Hessian A which can be expressed in terms of the Jacobian of the measurement function r , and we have $A \succeq 0$ [12]. Additionally, the relevant components of the matrix A for estimating the marginals for a subset of variables C_j can be recovered from its square root, i.e. the *square-root information matrix* (cf. [23]).

V. EXAMPLE APPLICATIONS

In the following sections we provide three example applications motivated by typical robot perception problems. In Section V-A, we begin with an instructive example formulating the classical problem of *point-cloud registration* in terms of a discrete-continuous factor graph, which can be optimized using our solver. In Section V-B, we consider the problem of *robust pose graph optimization*, in which we aim to estimate a set of poses given only noisy measurements between a subset of them, and where some fraction of those measurements may be outliers. We implement a straightforward approach to solving this problem using DC-SAM and show that it produces competitive results. Finally, in Section V-C, we demonstrate the application of our solver to a tightly-coupled semantic SLAM problem, where the variables of interest are robot poses, landmark locations, and semantic classes of each landmark.

A. Point-cloud registration

As a simple first example, we will consider the point-cloud registration problem. Consider a source point-cloud $\mathcal{P}_S = \{p_i^S \in \mathbb{R}^d, i = 1, \dots, n\}$ and target point-cloud $\mathcal{P}_T = \{p_j^T \in \mathbb{R}^d, j = 1, \dots, m\}$. Associate with each point in the source cloud p_i^S a discrete variable $d_i \in \{1, \dots, m\}$ determining the corresponding point in the target cloud. The goal of point-cloud registration is to identify the rigid-body transformation $T \in \text{SE}(3)$ that minimizes the following objective:

$$\min_{T \in \text{SE}(3)} \sum_{i=1}^n \|Tp_i^S - p_{d_i}^T\|_2^2. \quad (16)$$

The key challenge encountered in this setting is that the correspondence variables d_i are unknown and unobserved. We might consider, then, introducing the correspondence variables into the optimization, to determine the *best* set of correspondence variables *and* the corresponding rigid-body transformation of the point-cloud, obtaining the following problem:

$$\min_{d_i \in \{1, \dots, m\}, T \in \text{SE}(3)} \sum_{i=1}^n \|Tp_i^S - p_{d_i}^T\|_2^2. \quad (17)$$

Outliers (%)		Initial	LM	Ours	GNC [49]
100 (4%)	Cost	1.3×10^6	1.5×10^5	675.74	675.74
	Time (s)	-	20	14.5	52.7
1000 (29%)	Cost	1.3×10^6	5.1×10^5	675.74	675.74
	Time (s)	-	80	78.9	450
3000 (55%)	Cost	1.3×10^6	9.5×10^5	675.74	675.74
	Time (s)	-	108	145.9	1598

TABLE I: **Sphere dataset comparison.** Objective value (cost), and time required to compute SLAM solutions for our method, Levenberg-Marquardt (with outliers), and GNC [49]. Here cost refers to the objective value to be optimized as is computed with respect to *only* the inlier edges (so that the total cost reflects agreement with the inlier measurements). The initialization is computed from odometry and is independent of the outlier measurements.

Unfortunately, this problem is nonconvex and solving it to global optimality is, in general, NP-hard, requiring search over $\mathcal{O}(n^m)$ discrete state assignments.

A popular algorithm for solving the problem in equation (17) is to first posit an initial guess for the transformation T , determine the transformed locations of each of the points in the source cloud, then associate each point in the source cloud with the *nearest* point in the target cloud after the transformation. This is the *iterative closest point* (ICP) algorithm [3, 6]. Defining $r_i(T, d_i) = Tp_i^S - p_{d_i}^T$, we can see that the problem in equation (17) is concisely described in terms of factors of the form (3). Moreover, the conditional independence structure of the graph corresponding to this problem (depicted in Figure 1) immediately motivates our alternating optimization approach, since each d_i in fact *decouples* when conditioned on T . Finally, one can verify that our alternating optimization procedure turns out to be identical to ICP (as described above) in this setting. To demonstrate this fact, we applied our method to point cloud registration using the *Stanford Dragon* dataset [9], the results of which are depicted in Figure 3a. Indeed, we observe that our approach produces qualitatively reasonable results in just a few iterations. Moreover, while implementing ICP typically requires that we explicitly write the (independent) correspondence updates and transform update, we need not encode this explicitly at all: the fact that the discrete (correspondence) update separates into independent subproblems is simply a consequence of the conditional independence structure of the factor graph model in Figure 1c. That said, our approach does not have knowledge about the particular *spatial* structure of the problem and therefore performs naïve search over discrete assignments. In contrast, a typical implementation of ICP would make use of efficient spatial data structures to speed up the solution to the discrete subproblem, see [40] (indeed, such optimizations for *particular* problems like this would make for interesting future applications of the DC-SAM library). However, unlike any *particular* ICP implementation, our solver can be readily extended (without modification) to more complex cost functions or models because the structure of the subproblems is dictated by the independence structure inherent in the graphical model.

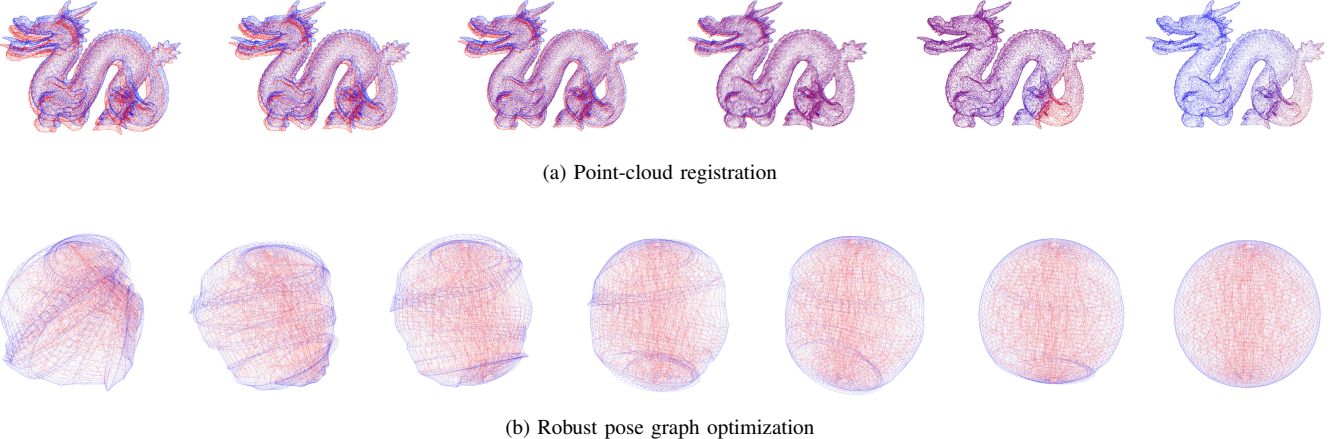


Fig. 3: **Example applications.** (a) Point-cloud registration using the *Stanford Dragon* dataset [9]. (b) Robust pose graph optimization using the *Sphere* dataset [24]. Each row displays the sequence of iterates for our method. In each case, we obtain high-quality solutions in just a few iterations.

Outliers (%)		Initial	LM	Ours	GNC [49]
10 (0.2%)	Cost	8363	220.1	0.63	0.63
	Time (s)	-	5.6	7.3	18.8
50 (1%)	Cost	8363	4419	2.67	1.65
	Time (s)	-	4.3	18	61.9
100 (2%)	Cost	8363	10268	3.22	2.19
	Time (s)	-	13.8	33.2	124

TABLE II: **Garage dataset comparison.** Objective value (cost), and time required to compute SLAM solutions for our method, Levenberg-Marquardt (with outliers) and GNC [49].

B. Robust Pose Graph Optimization

Next, we will consider robust pose graph optimization. In pose graph optimization are interested in estimating a set of poses $x_1, \dots, x_n \in \text{SE}(3)$ from noisy measurements \tilde{x}_{ij} of a subset of their (true) relative transforms $x_{ij} = x_i^{-1}x_j$. This problem possesses a natural graphical structure $\mathcal{G} = \{\mathcal{V}, \vec{\mathcal{E}}\}$ where nodes correspond to the poses x_i to be estimated and edges correspond to the available noisy measurements between them. Pose graph optimization then aims to solve the following problem:

$$\min_{x_i \in \text{SE}(3)} \sum_{\{i,j\} \in \vec{\mathcal{E}}} \underbrace{\|\text{Log}(\tilde{x}_{ij}^{-1}x_i^{-1}x_j)\|_{\Sigma}^2}_{r_{ij}(x_i, x_j)}, \quad (18)$$

where $\text{Log} : \text{SE}(3) \rightarrow \mathbb{R}^6$ takes an element of $\text{SE}(3)$ to an element of the tangent space, and $\Sigma \in \mathbb{R}^{6 \times 6}$ is a covariance matrix.

Suppose however, that some fraction of our measurements are corrupted by an unknown outlier process. We would like to determine the subset of outlier measurements and inlier measurements, as well as the corresponding optimal poses. It is typical to assume that the edges $\vec{\mathcal{E}}$ partition into a set of trusted odometry edges $\vec{\mathcal{E}}_{\mathcal{O}}$ and a set of untrusted loop closure edges $\vec{\mathcal{E}}_{\mathcal{L}}$. It is common to address this problem by introducing binary variables $d_{ij} \in \{0, 1\}$ for each of the untrusted edges (cf. [33, 44, 1, 42]), where $d_{ij} = 1$ indicates that the measurement \tilde{x}_{ij} is drawn from the outlier process. Since the outlier distribution

is unknown, it is common to assume that the outlier generating process is Gaussian with covariance $\tilde{\Sigma} \succ \Sigma$ much larger than the inlier model covariance. In turn, the problem of interest can be posed as follows:

$$\min_{x_i \in \text{SE}(3)} \sum_{\{i,j\} \in \vec{\mathcal{E}}} \|r_{ij}(x_i, x_j)\|_{\Sigma}^2 + \sum_{\{i,j\} \in \vec{\mathcal{E}}_{\mathcal{L}}} e_{ij}(x_i, x_j, d_{ij}), \quad (19)$$

where

$$e_{ij}(x_i, x_j, d_{ij}) \triangleq \begin{cases} -\log \omega_0 + \|r_{ij}(x_i, x_j)\|_{\Sigma}^2, & d_{ij} = 0, \\ -\log \omega_1 + \|r_{ij}(x_i, x_j)\|_{\Sigma}^2, & d_{ij} = 1, \end{cases} \quad (20)$$

and $\omega_0, \omega_1 \in [0, 1]$ are prior weights on the inlier and outlier hypotheses, respectively. Though they need not be normalized, one usually takes $\omega_0 = 1 - \omega_1$. Letting $|\vec{\mathcal{E}}_{\mathcal{L}}| = m$, there are $\mathcal{O}(2^m)$ possible assignments to the discrete variables in this problem. However, the above formulation can easily be represented in terms of discrete factors for the weights ω_0, ω_1 and discrete-continuous factors of the form in (3) to switch between the Gaussian inlier and outlier hypotheses. Moreover, once again, the discrete variables decouple from one another conveniently when we condition on an assignment to the continuous variables.

In our experimental setup, we corrupt a pose graph with outliers generated according to a similar process to the one described in [46, Section VI.C]: we randomly select a pair of (non-adjacent) poses and generate a loop closure with relative translation sampled uniformly from a cube of side-length 10 meters and rotation sampled from the uniform distribution on $\text{SO}(3)$.⁴ Based on the prior work of Olson and Agarwal [33], we selected $\omega_1 = 10^{-7}$ (with $\omega_0 = 1 - 10^{-7}$), and we made the outlier covariance model isotropic with variance 1.6×10^7 . We provide two points of comparison: a Levenberg-Marquardt (LM) solver applied to the graph corrupted by

⁴Our experimental setup differs from Tzoumas et al. [46] only in that they sample translations from within a ball of radius 5 meters.

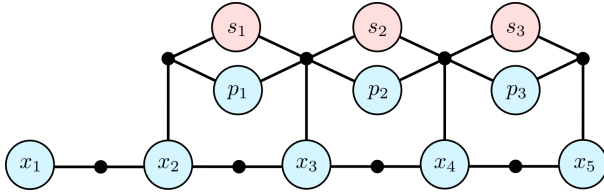


Fig. 4: **Factor graph representing semantic SLAM.** Here robot poses x_i are connected by odometry measurements, and joint geometric-semantic measurements are made between poses and landmarks (p_j, s_j). Measurements with multiple possible associations, represented as mixture factors in (21), are connected to multiple landmarks. To avoid clutter, the measurements depicted have only two hypotheses at most, but we allow for larger hypothesis sets in our implementation.

outliers (as a “worst case”) and the state-of-the-art graduated nonconvexity (GNC) solver [49].⁵ Table I summarizes our results on the *Sphere* dataset [24]. We provide the cost of each solution as obtained from the model containing *only inliers* (odometry and uncorrupted loop closures). In this sense, the reported cost reflects agreement of a given estimate with the inliers. We observe that across several configurations, our approach produces solutions attaining the same cost as GNC, but often *faster* than the non-robust solver (which does not reason about any discrete variables). Iterations of our method are fast, and we empirically observe convergence (established once an iterate of our approach no longer decreases the objective in (19)) in just a few iterations (see Figure 3 for qualitative results).⁶ We also tested each approach on the *Garage* dataset [19], which is considerably harder. Results of these experiments are summarized in Table II. All of the methods we considered break down after only relatively few outliers are added. In part, this demonstrates the sensitivity of these methods to the initial configuration, which is a key limitation of local optimization techniques (see Section VI for a more detailed discussion).

C. Tightly-coupled Semantic SLAM

Several recent works have considered the problem of jointly inferring a robot’s trajectory and a set of landmark positions and classes with unknown measurement correspondences, i.e. semantic SLAM [14, 5]. In particular, here we apply our approach to optimize jointly for robot poses $x_i \in \text{SE}(3), i = 1, \dots, n$, and landmark locations and classes $\ell_j = (p_j, s_j), p_j \in \mathbb{R}^3, s_j \in \mathcal{C}, j = 1, \dots, m$, where \mathcal{C} is an *a priori* known set of discrete semantic classes.

We adopt the general methodology of Doherty et al. [14] for data association: given a range-bearing measurement and associated semantic class obtained from an object detector,

⁵We use the GNC approach implemented in GTSAM with the truncated least-squares cost and an inlier cost threshold of 4 on *Sphere*, roughly half the default value, and 0.5 on *Garage*; we found that this gave the best performance for GNC, allowing it to serve as an “optimistic” baseline. We use the default stopping criterion.

⁶We also recovered discrete marginals as in equation (12a) and provide high-resolution visualizations in the supplement.

Method / Metric	Translation Error (m)		Rotation Error (deg)	
	Mean	RMSE	Mean	RMSE
VISO2 [17]	6.227	7.2772	2.489	2.735
Ours	2.175	2.442	1.486	1.665

TABLE III: **KITTI Seq 05.** Absolute translation and rotation errors (in meters and degrees, respectively) for our approach and VISO2 odometry.

we apply a threshold on the measurement likelihood to determine whether the measurement corresponds to a *new* or *old* landmark (for this, we employ the approximate marginal computations in (12a) and (15)). If it is a new landmark, we simply add the new measurement and landmark to our graph. If it is an old landmark, we add it to the graph as a mixture with a single component for each landmark that passes the likelihood threshold:

$$f_k(x_i, \mathcal{H}_k) \triangleq \max_{\ell_j \in \mathcal{H}_k} f_k(x_i, \ell_j), \quad (21)$$

where $\mathcal{H}_k \subseteq L$ is a subset of landmarks and the landmark measurement factor $f_k(x_i, \ell_j)$ decomposes as:

$$f_k(x_i, \ell_j) \triangleq \phi_k(s_j) \psi_k(x_i, p_j). \quad (22)$$

Here $\phi_k(s_j)$ is a categorical distribution and $\psi_k(x_i, p_j)$ is Gaussian with respect to the range and bearing between x_i and p_j . We also incorporate odometry factors of the form used in (18).⁷ The overall graphical model specifying this problem is depicted in Figure 4. Since the measurement factors in equation (22) involve both continuous and discrete variables, it is nontrivial to implement this within any existing framework. In the hybrid factor graph representation, however, problems of this form admit a concise description and solution using discrete-continuous factors.

In this demonstration, we consider semantic SLAM using stereo camera data from the KITTI dataset [18]. We sample keyframes every two seconds, using VISO2 [17] to obtain stereo odometry measurements and YOLO [35] for noisy detections of two types of objects: *cars* and *trucks*. We estimate the range and bearing to an object’s position as that of the median depth point projecting into a detected object’s bounding box. Using DC-SAM, we are able to compute solutions to this problem online in *real-time*.⁸ In Figure 5, we give a qualitative comparison of the trajectory computed using our approach and that of the VISO2 odometry. Table III gives a quantitative comparison. Our approach substantially improves upon the odometric estimate and additionally enables the estimation of discrete landmark classes.

VI. DISCUSSION

A. When is alternating minimization efficient?

The conditional factorization in equation (4) serves to give some intuition for when our optimization approach is computationally efficient. If the distribution over discrete variables

⁷For a more detailed exposition of this approach, see [14].

⁸We run our solver on an Intel i7 2.6 GHz CPU.

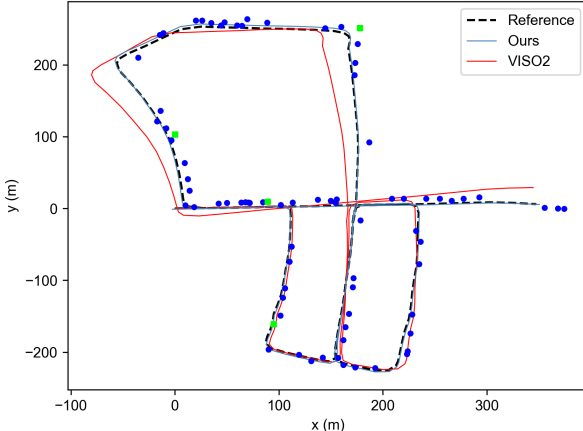


Fig. 5: **KITTI Seq 05.** Estimated trajectory (blue) compared to the ground truth (black, dashed) on the KITTI dataset sequence 05 using our semantic SLAM implementation. Blue circles are car landmarks, green squares are trucks.

conditioned on the continuous assignment admits a factorization into small subsets D_j , then the optimization problem in (8a) decouples into separate problems in direct correspondence with each set D_j . Since we perform exact inference on this distribution, solving for the most probable assignment is in the worst case exponential in the size of D_j [25]. Consequently, in graphs with densely connected discrete variables that are not decoupled by continuous variables, the per iteration complexity of alternating minimization can increase dramatically. That said, Proposition 1 ensures monotonic improvement in the objective so long as each optimization subproblem admits a solution no worse than the current iterate. Therefore, it is reasonable to consider extending this approach by allowing for *local* optimization in the discrete subproblem [41].

B. When can we ensure accurate solutions?

Though we are able to make some claims about when solutions to the discrete and continuous subproblems in our alternating minimization approach can be tractably computed, the question remains as to when one can ensure that these local search methods recover *high-quality* solutions. Since the alternating minimization approach is a *descent* method, we rely on the ability to provide a “good” initial guess from which purely going “downhill” in the cost landscape is enough to obtain a high-quality estimate. However, this is already a requirement of off-the-shelf tools for solving many robot perception problems, such as pose-graph SLAM, which (by virtue of the nonconvexity of the optimization problems they attempt to solve) require high-quality initialization [39]. Nonetheless, the consideration of discrete variables *can* make initialization more challenging. The specifics of providing an initial guess will ultimately depend heavily on the application.

One can also attempt to reduce the sensitivity of solutions obtained by a local optimization approach to initialization. A number of methods along these lines have been proposed. For

example, graduated nonconvexity (GNC) [49] as discussed in Section V-B, optimizes nonconvex functions by successively producing (and optimizing) a more well-behaved (typically convex) surrogate. Sampling methods and simulated annealing methods can improve convergence by allowing for the exploration of states that may *increase* cost or by initializing a descent method like our proposed approach from several starting points [28, 45]. Similarly, stochastic gradient descent is a classical approach for nonconvex optimization (and has appeared in the setting of robust pose-graph SLAM [32]), which could reasonably be adapted to our approach. Finally, heuristics have been considered which use consistency of measurements to filter out unlikely hypotheses [29] or to *re-initialize* estimates for factor graphs [27].

VII. CONCLUSION

In this work we presented an approach to optimization in discrete-continuous graphical models based on *alternating minimization*. Our key insight is that the structure of the alternating optimization procedure allows us to leverage the conditional independence relations exposed by factor graphs to efficiently perform local search. We showed how the complexity of inference in this setting is related to structure of the graphical model itself. Critically, we observed that many important problems in robotics can be framed in terms of graphical models admitting particularly advantageous structures for application of our approach. We provided a method for addressing the issue of recovering uncertainties associated with estimates in the discrete-continuous setting. Our solver and associated tools are implemented as part of our library, DC-SAM, which is, to the best of our knowledge, the first openly available library for addressing these *hybrid* discrete-continuous optimization problems. Finally, we demonstrate the application of our methods to several important robot perception problems: point-cloud registration, robust pose graph optimization, and semantic SLAM.

REFERENCES

- [1] Pratik Agarwal, Gian Diego Tipaldi, Luciano Spinello, Cyrill Stachniss, and Wolfram Burgard. Robust map optimization using dynamic covariance scaling. In *2013 IEEE International Conference on Robotics and Automation*, pages 62–69. Ieee, 2013.
- [2] Sameer Agarwal and Keir Mierle. *Ceres Solver: Tutorial & Reference*. Google Inc.
- [3] Paul J Besl and Neil D McKay. Method for registration of 3-D shapes. In *Sensor Fusion IV: Control Paradigms and Data Structures*, volume 1611, pages 586–606. International Society for Optics and Photonics, 1992.
- [4] Christopher M. Bishop. *Pattern Recognition and Machine Learning*. Springer, 2006.
- [5] Sean L Bowman, Nikolay Atanasov, Kostas Daniilidis, and George J Pappas. Probabilistic data association for semantic SLAM. In *International Conference on Robotics and Automation (ICRA)*, pages 1722–1729, 2017.
- [6] Yang Chen and Gérard Medioni. Object modelling by registration of multiple range images. *Image and vision computing*, 10(3):145–155, 1992.
- [7] Contributors, Ecosystem, and NavAbility. Caesar.jl, v0.11.1, 2021. <https://github.com/JuliaRobotics/Caesar.jl>.

- [8] Ingemar J Cox and John J Leonard. Modeling a dynamic environment using a Bayesian multiple hypothesis approach. *Artificial Intelligence*, 66(2):311–344, 1994.
- [9] Brian Curless and Marc Levoy. A volumetric method for building complex models from range images. In *Proceedings of the 23rd Annual Conference on Computer Graphics and Interactive Techniques*, pages 303–312, 1996.
- [10] Frank Dellaert. Factor graphs and GTSAM: A hands-on introduction. Technical report, Georgia Institute of Technology, 2012.
- [11] Frank Dellaert. Factor graphs: Exploiting structure in robotics. *Annual Review of Control, Robotics, and Autonomous Systems*, 4(1):141–166, 2021. doi: 10.1146/annurev-control-061520-010504. URL <https://doi.org/10.1146/annurev-control-061520-010504>.
- [12] Frank Dellaert, Michael Kaess, et al. Factor graphs for robot perception. *Foundations and Trends® in Robotics*, 6(1-2):1–139, 2017.
- [13] Arthur P Dempster, Nan M Laird, and Donald B Rubin. Maximum likelihood from incomplete data via the EM algorithm. *Journal of the Royal Statistical Society: Series B (Methodological)*, 39(1):1–22, 1977.
- [14] Kevin Doherty, David Baxter, Edward Schneeweiss, and John J. Leonard. Probabilistic data association via mixture models for robust semantic SLAM. In *International Conference on Robotics and Automation (ICRA)*, 2020.
- [15] Dehann Fourie, John Leonard, and Michael Kaess. A nonparametric belief solution to the Bayes tree. In *2016 IEEE/RSJ International Conference on Intelligent Robots and Systems (IROS)*, pages 2189–2196. IEEE, 2016.
- [16] Caelan Reed Garrett, Rohan Chitnis, Rachel Holladay, Beomjoon Kim, Tom Silver, Leslie Pack Kaelbling, and Tomás Lozano-Pérez. Integrated Task and Motion Planning. *Annual Review of Control, Robotics, and Autonomous Systems*, 4(1):265–293, 2021. doi: 10.1146/annurev-control-091420-084139. URL <https://doi.org/10.1146/annurev-control-091420-084139>.
- [17] Andreas Geiger, Julius Ziegler, and Christoph Stiller. Stereo-Scan: Dense 3d Reconstruction in Real-time. In *IEEE Intelligent Vehicles Symposium*, Baden-Baden, Germany, June 2011.
- [18] Andreas Geiger, Philip Lenz, Christoph Stiller, and Raquel Urtasun. Vision meets Robotics: The KITTI Dataset. *International Journal of Robotics Research (IJRR)*, 2013.
- [19] Giorgio Grisetti, Rainer Kümmerle, Hauke Strasdat, and Kurt Konolige. g2o: A general framework for (hyper) graph optimization. In *Proceedings of the IEEE International Conference on Robotics and Automation (ICRA)*, pages 9–13, 2011.
- [20] Ming Hsiao and Michael Kaess. MH-iSAM2: Multi-hypothesis iSAM using Bayes tree and hypo-tree. In *2019 International Conference on Robotics and Automation (ICRA)*, pages 1274–1280. IEEE, 2019.
- [21] Qiangqiang Huang, Can Pu, Dehann Fourie, Kasra Khosoussi, Jonathan P How, and John J Leonard. NF-iSAM: Incremental Smoothing and Mapping via Normalizing Flows. *arXiv preprint arXiv:2105.05045*, 2021.
- [22] Fan Jiang, Varun Agrawal, Russell Buchanan, Maurice Fallon, and Frank Dellaert. iMHS: An Incremental Multi-Hypothesis Smoother. *arXiv preprint arXiv:2103.13178*, 2021.
- [23] M. Kaess and F. Dellaert. Covariance recovery from a square root information matrix for data association. *J. of Robotics and Autonomous Systems*, 57(12):1198–1210, December 2009. doi: 10.1016/j.robot.2009.06.008.
- [24] M. Kaess, H. Johannsson, R. Roberts, V. Ila, J. J. Leonard, and F. Dellaert. iSAM2: Incremental smoothing and mapping using the Bayes tree. *The International Journal of Robotics Research*, 31:217–236, February 2012.
- [25] D. Koller and N. Friedman. *Probabilistic Graphical Models: Principles and Techniques*. The MIT Press, Cambridge, MA, 2009.
- [26] Pierre-Yves Lajoie, Siyi Hu, Giovanni Beltrame, and Luca Carlone. Modeling perceptual aliasing in SLAM via discrete-continuous graphical models. *IEEE Robotics and Automation Letters*, 4(2):1232–1239, 2019.
- [27] Ziqi Lu, Qiangqiang Huang, Kevin Doherty, and John J. Leonard. Consensus-Informed Optimization Over Mixtures for Ambiguity-Aware Object SLAM. In *2021 IEEE/RSJ International Conference on Intelligent Robots and Systems (IROS)*. IEEE, 2021.
- [28] David John Cameron Mackay. Introduction to Monte Carlo Methods. In *Learning in graphical models*, pages 175–204. Springer, 1998.
- [29] Joshua G Mangelson, Derrick Dominic, Ryan M Eustice, and Ram Vasudevan. Pairwise consistent measurement set maximization for robust multi-robot map merging. In *2018 IEEE International Conference on Robotics and Automation (ICRA)*, pages 2916–2923. IEEE, 2018.
- [30] Michael Montemerlo and Sebastian Thrun. Simultaneous localization and mapping with unknown data association using fastSLAM. In *2003 IEEE International Conference on Robotics and Automation*, volume 2, pages 1985–1991. IEEE, 2003.
- [31] José Neira and Juan D Tardós. Data association in stochastic mapping using the joint compatibility test. *IEEE Transactions on robotics and automation*, 17(6):890–897, 2001.
- [32] E. Olson, J. Leonard, and S. Teller. Fast iterative alignment of pose graphs with poor initial estimates. In *IEEE International Conference on Robotics and Automation*, pages 2262–2269, May 2006.
- [33] Edwin Olson and Pratik Agarwal. Inference on networks of mixtures for robust robot mapping. *The International Journal of Robotics Research*, 32(7):826–840, 2013.
- [34] Tim Pfeifer, Sven Lange, and Peter Protzel. Advancing Mixture Models for Least Squares Optimization. *IEEE Robotics and Automation Letters*, 6(2):3941–3948, 2021.
- [35] Joseph Redmon, Santosh Divvala, Ross Girshick, and Ali Farhadi. You only look once: Unified, real-time object detection. In *Proceedings of the IEEE conference on computer vision and pattern recognition*, pages 779–788, 2016.
- [36] Donald Reid. An algorithm for tracking multiple targets. *IEEE transactions on Automatic Control*, 24(6):843–854, 1979.
- [37] David M Rosen, Michael Kaess, and John J Leonard. An incremental trust-region method for robust online sparse least-squares estimation. In *Robotics and Automation (ICRA), 2012 IEEE International Conference on*, pages 1262–1269. IEEE, 2012.
- [38] David M Rosen, Michael Kaess, and John J Leonard. Robust incremental online inference over sparse factor graphs: Beyond the Gaussian case. In *2013 IEEE International Conference on Robotics and Automation*, pages 1025–1032. IEEE, 2013.
- [39] David M Rosen, Kevin J Doherty, Antonio Terán Espinoza, and John J Leonard. Advances in Inference and Representation for Simultaneous Localization and Mapping. *Annual Review of Control, Robotics, and Autonomous Systems*, 4(1):215–242, 2021. doi: 10.1146/annurev-control-072720-082553. URL <https://doi.org/10.1146/annurev-control-072720-082553>.
- [40] Szymon Rusinkiewicz and Marc Levoy. Efficient variants of the ICP algorithm. In *Proceedings of the Third International Conference on 3-D Digital Imaging and Modeling*, pages 145–152. IEEE, 2001.
- [41] Bogdan Savchynskyy et al. Discrete graphical models—an optimization perspective. *Foundations and Trends® in Computer Graphics and Vision*, 11(3-4):160–429, 2019.
- [42] Aleksandr V Segal and Ian D Reid. Hybrid inference optimization for robust pose graph estimation. In *Intelligent Robots and Systems (IROS 2014), 2014 IEEE/RSJ International Conference on*, pages 2675–2682. IEEE, 2014.

- [43] Erik B Sudderth, Alexander T Ihler, Michael Isard, William T Freeman, and Alan S Willsky. Nonparametric belief propagation. *Communications of the ACM*, 53(10):95–103, 2010.
- [44] Niko Sünderhauf and Peter Protzel. Switchable constraints for robust pose graph SLAM. In *Intelligent Robots and Systems (IROS), 2012 IEEE/RSJ International Conference on*, pages 1879–1884. IEEE, 2012.
- [45] Harold Szu and Ralph Hartley. Fast simulated annealing. *Physics letters A*, 122(3-4):157–162, 1987.
- [46] Vasileios Tzoumas, Pasquale Antonante, and Luca Carlone. Outlier-robust spatial perception: Hardness, general-purpose algorithms, and guarantees. In *2019 IEEE/RSJ International Conference on Intelligent Robots and Systems (IROS)*, pages 5383–5390. IEEE, 2019.
- [47] Andrew Viterbi. Error bounds for convolutional codes and an asymptotically optimum decoding algorithm. *IEEE Transactions on Information Theory*, 13(2):260–269, 1967.
- [48] Jinkun Wang and Brendan Englot. Robust exploration with multiple hypothesis data association. In *2018 IEEE/RSJ International Conference on Intelligent Robots and Systems (IROS)*, pages 3537–3544. IEEE, 2018.
- [49] Heng Yang, Pasquale Antonante, Vasileios Tzoumas, and Luca Carlone. Graduated non-convexity for robust spatial perception: From non-minimal solvers to global outlier rejection. *arXiv preprint arXiv:1909.08605*, 2019.